

Notes

Splat: A Nonequilibrium Morphology on the Way to a Microemulsion

Emmanuel Girard-Reydet* and
Jean-Pierre Pascault

Laboratoire des Matériaux Macromoléculaires-UMR
CNRS 5627, Institut National des Sciences Appliquées, 20,
Avenue A. Einstein, 69621 Villeurbanne Cedex, France

Hugh R. Brown*

BHP Steel Institute, University of Wollongong,
Wollongong, NSW 2522, Australia

Received December 29, 2000

Revised Manuscript Received March 13, 2001

Introduction

In the field of polymer blends, the emulsifying activity of diblock copolymers has been widely used to solve the problems associated with strong immiscibility namely, high interfacial tension, and poor interphase adhesion, which are thought to be the reason for poor mechanical properties.^{1–9} Theoretical models have been developed to describe the molecular mechanisms of emulsification or compatibilization by block copolymers.^{10,11} The loss of conformational entropy due to the segregation of the blocks to the interfaces is compensated by the gain in enthalpy as each block is in the corresponding compatible homopolymer phase so that the overall interfacial tension is decreased. Since the domain size in a polymer blend is strongly influenced by the interfacial tension, adding block copolymer to the interface makes the phase domains smaller.

If the driving force for interfacial segregation is high enough, the interfacial tension can be made to vanish and polymeric microemulsions similar to oil/water/surfactant microemulsions can be formed.^{12–16} Such microemulsions are difficult to obtain from an A/B immiscible blend by adding an A-*b*-B diblock copolymer. The achievement of a vanishing interfacial tension is then thermodynamically and kinetically limited by aggregation of the diblock copolymer chains in the bulk phases. Polymeric microemulsions can alternatively be obtained by adding an A-*b*-D or C-*b*-D diblock copolymer which have favorable enthalpic interactions with one or both of the homopolymer phases. These favorable thermodynamic interactions increase the driving force for interfacial segregation so that the interfacial tension can be driven to zero or slightly negative before the onset of micellization.¹² The morphological consequences of the vanishing of the interfacial tension have been directly visualized by transmission electron microscopy^{13,15,16} or scanning force microscopy¹⁶ in the case of A/B/A-*b*-D systems (with B interacting favorably with D) with an initially planar melt interface. The interface

becomes unstable, leading to spontaneous formation of a deeply corrugated interface and copolymer coated droplets nearby.

The aim of this note is to show how spectacular the morphological consequences may be of driving the interfacial tension to zero at an initially spherical interface in an appropriate reactive system. The immiscible blend investigated here is a thermoplastic/thermoset blend generated by reaction-induced phase separation. As the thermoplastic solution in the thermoset precursors is initially homogeneous, macroscopic phase separation is induced due to the decrease of the entropy of mixing caused by the increase in the molar mass of the growing thermoset. The final morphology in the resulting thermoplastic/thermoset blend (without diblock) is strongly dependent on the complex competition between phase separation rates and polymerization rates.^{17–25} In particular, considering the dynamics of phase separation, a chemical “quench” from the miscible one-phase region into the metastable or unstable region results in nucleation and growth or spinodal demixing, respectively. The complexity of these systems has led to a limited number of theoretical attempts to explain the phase separation behavior despite many experimental studies.

In the current work poly(phenylene ether) (PPE) was selected as the thermoplastic phase and an amine cured polyepoxide (DGEBA–MCDEA; see below) as the thermoset phase. The initial miscibility conditions, kinetics including gelation and vitrification, reaction-induced phase separation process, and final morphologies of this system have been already studied.^{17,18,23,24} The diblock copolymer was a symmetrical polystyrene-*block*-poly(methyl methacrylate) copolymer (PS-*b*-PMMA), chosen because (i) homoPS interacts very favorably and thus exhibits a negative interaction parameter with PPE ($\chi_{PS/PPE} = -0.1$)²⁶ and (ii) homoPMMA was recently shown to remain miscible with the (DGEBA–MCDEA) polyepoxide system during the whole curing process whatever the concentration and the temperature.²⁷

Experimental Section

Materials. The polyepoxide precursors were a classical diepoxy prepolymer, diglycidyl ether of bisphenol A (DGEBA), with a low average degree of polymerization ($n = 0.03$) and an aromatic diamine: 4,4'-methylenebis[3-chloro-2,6-diethyl-aniline] (MCDEA). The reactants were used as-received with a stoichiometric ratio epoxy to amino-hydrogen equal to unity.

The thermoplastic used in this work was a poly(phenylene ether) (PPE), PPE 800 supplied by General Electric.

The diblock copolymer was an extremely pure symmetrical polystyrene-*block*-poly(methyl methacrylate) copolymer (PS-*b*-PMMA), synthesized by anionic polymerization and supplied by Polymer Source.

An homopolystyrene (PS), with the same molar mass than that of the PS block in the diblock copolymer and supplied by Polymer Source, was used to investigate the solubility behavior of PS in DGEBA–MCDEA before and during isothermal reaction.

* To whom correspondence should be addressed.

Table 1. Chemical Structures and Characteristics of the Blend Components

Material	Formulae	Supplier	M_n (g.mol ⁻¹)	I_p	T_g (°C)
Diglycidyl ether of bisphenol A (DGEBA)		Dow Chemical DER332	348.5		
4,4'-methylenebis[3-chloro 2,6-diethylaniline] (MCDEA)		Lonza	380		
Polyphenylene ether (PPE)		General Electric PPE 800	26000	1.90	220
Polystyrene (PS)		Polymer Source	50000	1.03	
Polystyrene- <i>b</i> -polymethyl methacrylate (PS- <i>b</i> -PMMA)		Polymer Source	PS: 50000 PMMA: 54000	1.03	

The chemical structures and characteristics of the monomers, thermoplastics, and copolymer are listed in Table 1.

For the blend preparation, the diamine was added after complete dissolution of the thermoplastic and/or copolymer in DGEBA at 135 °C. The solution was then reacted at a fixed isothermal temperature, $T_i = 135$ °C, where it was initially homogeneous (see Results). To ensure that maximum extent of reaction-induced phase separation could occur, the reaction time was chosen greater than the vitrification time of the epoxy system.¹⁷

Techniques. Cloud point temperatures, T_{cp} , of PPE–DGEBA–MCDEA and of PS–DGEBA–MCDEA unreacted mixtures, containing different thermoplastic concentrations, were determined using a light transmission setup. Temperature was increased until a homogeneous solution was obtained, kept constant for several minutes, and then decreased at a cooling rate on the order of 1 °C min⁻¹. T_{cp} was determined as the onset temperature of the light transmission decrease. Substantial reactions did not take place during these measurements due to the very low reactivity of the selected DGEBA–MCDEA system.¹⁸

Polycondensation of PPE–DGEBA–MCDEA and of PS–DGEBA–MCDEA mixtures was carried out in the light transmission setup at $T_i = 135$ °C and the cloud-point time, t_{cp} , was determined as the onset time of the light transmission decrease. At this time the test tube was taken out of the device and chilled in ice. The epoxy conversion at the cloud point, x_{cp} , was determined using SEC.¹⁷

Transmission electron microscopy was used to obtain images of the cured binary and ternary blends. Ultrathin sections were prepared at room temperature. As no staining was necessary to obtain contrast between phases in the case of the blends containing PPE with or without PS-*b*-PMMA, ultrathin sections from the binary blend containing PS-*b*-PMMA without PPE were stained 2 min with ruthenium tetroxide (RuO₄) vapor. The PS blocks were then preferentially stained due to the oxidation of the aromatic rings.²⁸ Samples were imaged in a JEM-200CX transmission electron microscope with an accelerating voltage of 80 kV.

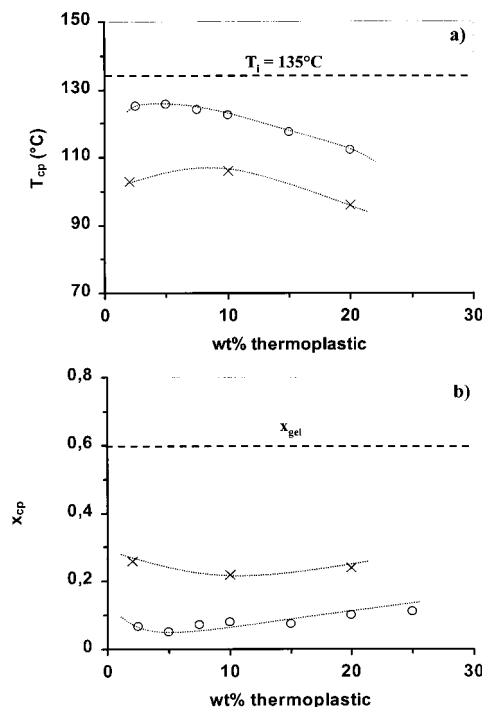


Figure 1. (a) Cloud point temperatures, T_{cp} , and (b) cloud point conversions, x_{cp} , vs mass fraction of PPE (○) and PS (×) in mixtures with DGEBA–MCDEA stoichiometric formulations, before and during reaction at $T_i = 135$ °C where any blend was initially homogeneous, respectively.

Results and Discussion

Figure 1a,b shows cloud-point temperatures, T_{cp} , and cloud-point conversions, x_{cp} , vs mass fraction of PPE and PS (same molar mass than that of the PS block in the diblock copolymer) in mixtures with DGEBA–MCDEA

stoichiometric formulations, before and during reaction at $T_i = 135^\circ\text{C}$ where any blend was initially homogeneous, respectively. Both systems are characterized by an upper critical solution temperature (UCST) behavior (i.e., miscibility increases with temperature). PS can be seen to be more miscible than PPE with the thermoset precursors, resulting in a higher extent of reaction at phase separation during isothermal cure. On the other hand, PMMA (higher molar mass than that of the PMMA block in the diblock copolymer) was recently shown to be initially miscible and remain completely miscible with DGEBA–MCDEA during the whole reaction process whatever the concentration and the temperature.

The micrograph in Figure 2a shows the domain structures of the binary blend containing 10 wt % PPE (without copolymer) after cure at $T_i = 135^\circ\text{C}$. The bright regions correspond to the polyepoxide-rich phase (α phase) and the dark parts to the thermoplastic-rich phase (β phase). Reaction-induced phase separation thus resulted in the formation of PPE-rich macroparticles, with sizes around $2\text{--}5\ \mu\text{m}$, dispersed in a continuous polyepoxide-rich matrix. For this thermoplastic concentration just lower than the critical composition ($c_{\text{crit}} = 11.4\ \text{wt}\%$),¹⁸ the macrophase separation process has been found to behave as follows:^{23,24} (i) The initial phase separation mechanism was spinodal demixing from the growth of concentration fluctuations. Because of the very low reactivity of the DGEBA–MCDEA system, spinodal demixing under nonisothermal conditions—the driving force for phase separation is continuously increased since the reaction continuously proceeds until vitrification is reached—was found to be very similar to the classical isothermal spinodal demixing. (ii) The initial high degree of interconnectivity was interrupted by the increase of the interfacial tension as both phases purified, resulting in a dispersed droplet-like morphology with dispersed β macrodomains. (iii) Because of the very low conversion at cloud point ($x_{\text{cp}} = 0.08$ located far before the gel conversion, x_{gel} being close to 0.6) and therefore the low viscosity of the blend at phase separation, considerable coalescence of the dispersed PPE-rich macroparticles could occur until they vitrified as their purity increased. (The glass transition temperature, T_g , of PPE was much higher than the chosen cure temperature.) Spherical secondary phase-separated regions of polyepoxide can also be seen within some PPE-rich domains. This behavior is typical of a blend that undergoes its first separation in the critical region of its phase diagram, i.e., in the unstable region, after spending no or a negligible amount of time in the metastable region. This phenomenon arises from the fact that, as phase separation proceeds, the thermoset within each phase also continues to cross-link. While these compositions of the phases are initially stable, the increase in the molar mass of the growing diepoxy–diamine copolymer may induce a secondary phase separation within one or both (in the case of bicontinuous) phases.²⁰

The binary blend containing 2 wt % PS-*b*-PMMA (without PPE) was transparent after cure at $T_i = 135^\circ\text{C}$, indicating no macrophase separation of thermoset and diblock copolymer in the final cured state. Only microphase separation occurred, as revealed by the high-magnification TEM image in Figure 2b exhibiting microparticles with diameters in the range of 30 nm. It is worth noting that, differently from the 10PPE blend,

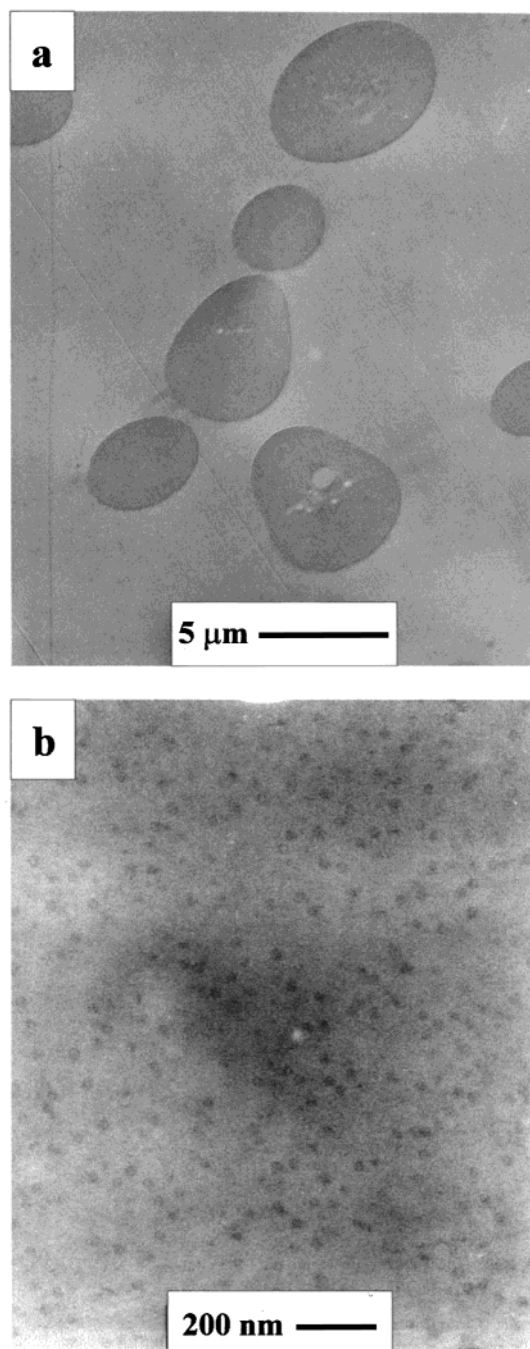


Figure 2. Transmission electron micrographs of the binary blends after cure at $T_i = 135^\circ\text{C}$: (a) 10 wt % PPE, without copolymer (low magnification: $\times 3000$); (b) 2 wt % PS-*b*-PMMA, without PPE (high magnification: $\times 45\,000$).

obtaining a phase contrast by TEM required the staining of ultrathin sections with ruthenium tetroxide (RuO_4), which was observed to preferentially stain the PS blocks, which appeared dark. During the curing process, at $x_{\text{cp(PS)}} = 0.26$, the initially soluble PS blocks undergo phase separation, and the reacting epoxy solvent becomes a selective solvent of PMMA blocks. The result is the formation of micelles consisting of a “core” of insoluble PS segments and a “corona” of soluble PMMA segments. Since PMMA blocks remain soluble within the growing thermoset until the end of the reaction, macrophase separation is prevented, and the final structure consists of discrete PS microdomains, compatibilized by the miscible PMMA blocks, in the polyepoxide matrix.

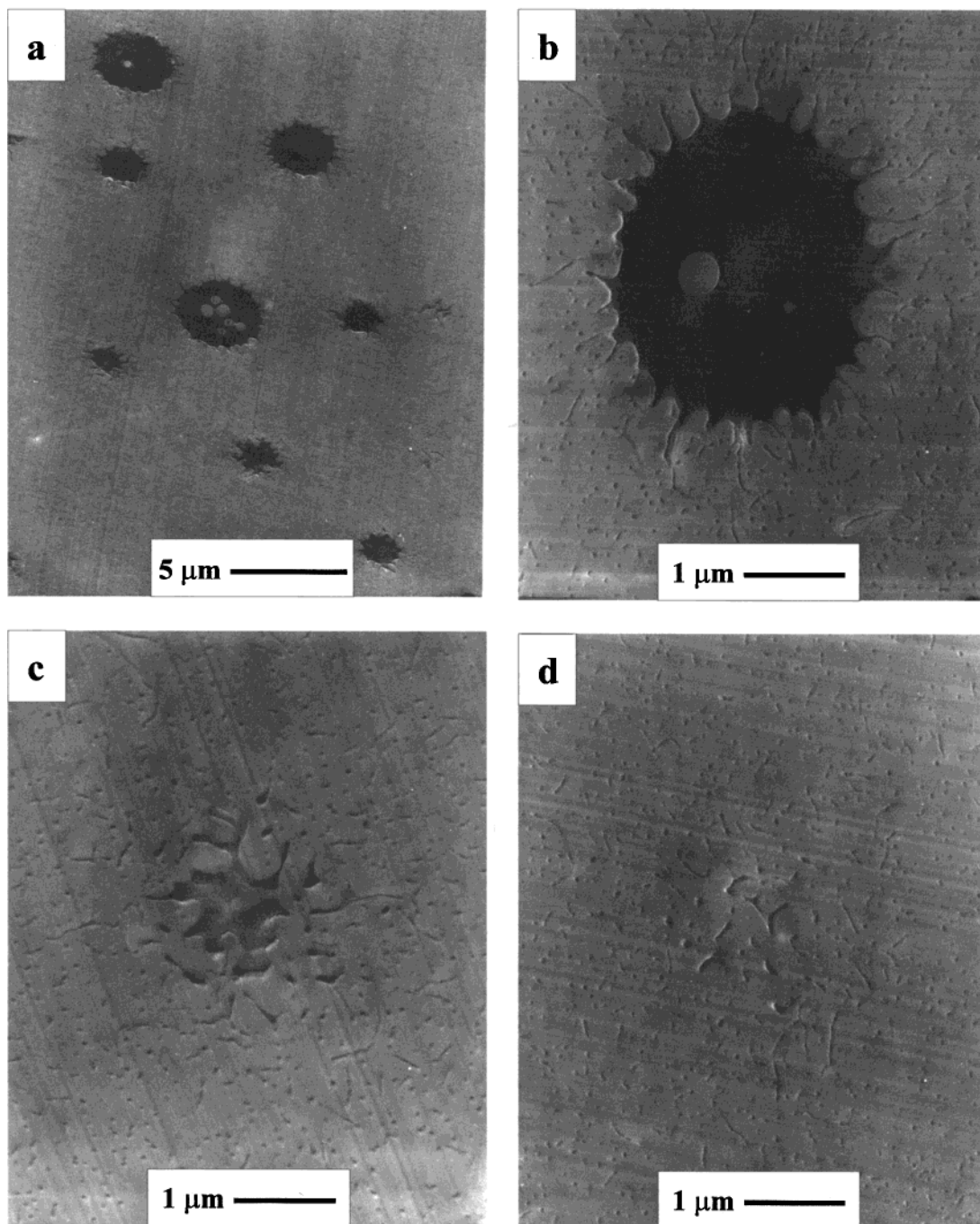


Figure 3. Transmission electron micrographs of the ternary blend containing 10 wt % PPE plus 2 wt % PS-*b*-PMMA after cure at $T_i = 135\text{ }^{\circ}\text{C}$, at two magnifications: (a) $\times 3000$; (b–d) $\times 13\,000$.

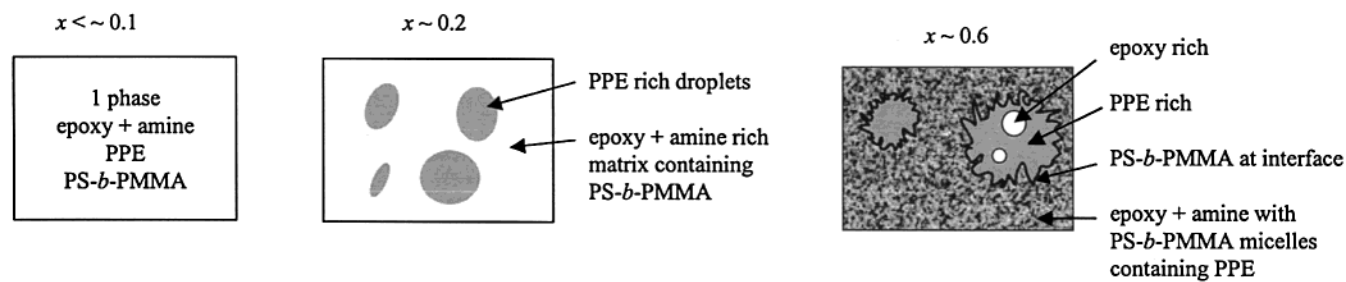


Figure 4. Schematics of the different stages of the demixing of the ternary blend containing 10 wt % PPE plus 2 wt % PS-*b*-PMMA during curing at $T_i = 135\text{ }^{\circ}\text{C}$.

The final morphology of the ternary blend containing 10 wt % PPE plus 2 wt % PS-*b*-PMMA is illustrated by the series of TEM images at two magnifications in

Figure 3a–d. The addition of diblock copolymer to the PPE/thermoset blend is thus shown to induce a change from a one-scale structure with spherical PPE-rich

macroparticles to a two-scale structure with complex "splat-like" PPE-rich macrodomains coexisting with filament-like and spherical microdomains. The PPE-rich phase was shown to macrophase separate at low cure and to be initially very impure, leading to the formation of internal polyepoxide-rich droplets. The fact that these internal droplets are not influenced by the diblock (see the spherical interface in micrograph b of Figure 3) is a strong indication that the PPE-rich phase does not contain copolymer. Until $x_{\text{cp(PS)}} (> x_{\text{cp(PPE)}})$ is reached, the diblock is mainly solubilized in the epoxy-rich phase and does not affect the coalescence process of the segregated PPE-rich domains, so that a macroscale structure could develop similarly to that in the blend without copolymer. At $x_{\text{cp(PS)}}$, the diblock microphase separates from the growing thermoset. Because of the very favorable interactions between PS blocks and PPE ($\chi_{\text{PS/PPE}} < 0$) on one hand and the miscibility of PMMA blocks with the growing polyepoxide on the other, the diblock is driven to the interface where it stops the coalescence of PPE-rich particles (domain sizes are significantly lower than those obtained without copolymer as can be seen by comparing micrographs in Figures 2a and 3a) and, when sufficient has accumulated, drives the interfacial tension negative. That negative tension then becomes the driving force for increasing the interfacial area. Therefore, the interface becomes unstable, and its area expands by the growth of fluctuations. As the reaction continues, the high- T_g blend vitrifies, thereby "freezing in" the out-of-equilibrium corrugated interface, resulting in the existence of spectacular "splat"-like PPE-rich domains shown in micrographs a and b of Figure 3. The large deformations of the interface cause emulsified filaments and droplets to break off from it, as revealed by the presence of microdomains near the splat-like domains and throughout the whole sample. It should be noted that these microparticles must consist of PPE dissolved in diblock micelles and not pure diblock micelles because they could be observed by TEM without staining. A comparison of micrographs b–d of Figure 3 provides evidence for the different stages in the copolymer-induced microemulsion process. The latter micrograph shows an area containing diblock-coated microfilaments and microdroplets, which presumably come from a PPE-rich macroparticle that has broken up and partially dissolved. Schematics of the different stages of the demixing of the ternary blend during curing at $T_i = 135^\circ\text{C}$ are drawn in Figure 4.

The work presented here demonstrates the profound effect that the presence of a diblock copolymer can have on the reaction-induced morphology of a thermoplastic–thermoset blend. Important drivers in obtaining the observed splat morphology are (i) that phase separation of the PPE occurred before phase separation of the diblock and (ii) that the PS block of the diblock is highly miscible with PPE while the PMMA block is miscible with the polyepoxide but highly immiscible with PPE. Addition of diblock to a thermoplastic–thermoset blend is shown to be a technique that can be used to obtain a

kinetically stabilized system with a very high interfacial area, and it may be possible to obtain a bicontinuous system by judicious choice to the blend composition. The effects of cure temperature will be described in a later publication as altering the cure temperature alters both reaction rates and reaction extent at morphological "freezing".

References and Notes

- (1) Gaillard, P.; Ossenbach, M.; Riess, G. *Makromol. Chem., Rapid Commun.* **1980**, *1*, 771.
- (2) Fayt, R.; Jerome, R.; Teyssier, P. J. *Polym. Sci. Phys.* **1981**, *19*, 1269.
- (3) Schwartz, M. C.; Barlow, J. W.; Paul, D. R. *J. Appl. Polym. Sci.* **1988**, *24*, 525.
- (4) Creton, C.; Kramer, E. J.; Hadziiaannou, G. *Macromolecules* **1991**, *24*, 1846.
- (5) Brown, H. R. *Macromolecules* **1991**, *24*, 2752.
- (6) Thomas, S.; Prud'homme, R. E. *Polymer* **1992**, *33*, 4260.
- (7) Auschra, C.; Stadler, R.; Voigt-Martin, I. *Polymer* **1993**, *34*, 2081; *Polymer* **1993**, *34*, 2093.
- (8) Adedji, A.; Jamieson, A. M. *Polymer* **1993**, *34*, 5038.
- (9) Creton, C.; Brown, H. R.; Deline, V. R. *Macromolecules* **1994**, *27*, 1774.
- (10) Leibler, L. *Macromolecules* **1982**, *15*, 1283; *Makromol. Chem., Makromol. Symp.* **1988**, *16*, 1.
- (11) Noolandi, J.; Hong, K. M. *Macromolecules* **1982**, *15*, 482; *Macromolecules* **1984**, *17*, 1531.
- (12) Shull, K. R.; Kelloch, A. J.; Deline, V. R.; MacDonald, S. A. *J. Chem. Phys.* **1992**, *97*, 2095.
- (13) Xu, Z.; Jandt, K. D.; Kramer, E. J.; Edgecombe, B. D.; Fréchet, J. M. J. *J. Polym. Sci., Polym. Phys.* **1995**, *33*, 2351.
- (14) Fredrickson, G. H.; Bates, F. S. *J. Polym. Sci., Polym. Phys.* **1997**, *35*, 2775.
- (15) Bates, F. S.; Maurer, W. W.; Lipic, P. M.; Hillmeyer, M. A.; Almdal, K.; Mortensen, K.; Fredrickson, G. H.; Lodge, T. P. *Phys. Rev. Lett.* **1997**, *79*, 849.
- (16) Jiao, J.; Kramer, E. J.; de Vos, S.; Möller, M.; Koning, C. *Macromolecules* **1999**, *32*, 6261.
- (17) Girard-Reydet, E.; Riccardi, C. C.; Sautereau, H.; Pascault, J. P. *Macromolecules* **1995**, *28*, 7599; *Macromolecules* **1995**, *28*, 7608.
- (18) Riccardi, C. C.; Borrajo, J.; Williams, R. J. J.; Girard-Reydet, E.; Sautereau, H.; Pascault, J. P. *J. Polym. Sci., Polym. Phys.* **1996**, *34*, 349.
- (19) Ohnaga, T.; Chen, W.; Inoue, T. *Polymer* **1994**, *35*, 3774.
- (20) Clarke, N.; McLeish, T. C. B.; Jenkins, S. D. *Macromolecules* **1995**, *28*, 4650.
- (21) Elliniadis, S.; Higgins, J. S.; Clarke, N.; McLeish, T. C. B.; Choudhery, R. A.; Jenkins, S. D. *Polymer* **1997**, *38*, 4855.
- (22) Elicabe, G. E.; Larrondo, H. A.; Williams, R. J. J. *Macromolecules* **1997**, *30*, 6550.
- (23) Girard-Reydet, E.; Sautereau, H.; Pascault, J. P.; Keates, P.; Navard, P.; Thollet, G.; Vigier, G. *Polymer* **1998**, *39*, 2269.
- (24) Girard-Reydet, E.; Sautereau, H.; Pascault, J. P. *Polymer* **1999**, *40*, 1677.
- (25) Pascault, J. P.; Williams, R. J. J. In *Polymer Blends. 1-Formulation*; Paul, D. R., Bucknall, C. B., Eds.; 2000; p 379.
- (26) Kambour, R. P.; Bendler, J. T.; Boop, R. D. *Macromolecules* **1983**, *16*, 753.
- (27) Ritzenthaler, S.; Girard-Reydet, E.; Pascault, J. P. *Polymer* **2000**, *41*, 6375.
- (28) Trent, J. S.; Scheinbeim, J. I.; Couchman, P. R. *J. Polym. Sci., Polym. Lett. Ed.* **1981**, *19*, 315; *Macromolecules* **1983**, *16*, 589.

MA002241X